# Supplementary Materials for

## Rapid clay precipitation in explosion-induced fractures

Erika Swanson*, Aviva Sussman, Jennifer Wilson

*correspondence to: emswanson@lanl.gov

**This PDF file includes:**

Detailed methods
Table DR1
Figure DR1

**Detailed Methods**

Each thin section was prepared from billets cut with a standard rock saw using standard tap water for cooling. Each thin section was finished to a 30 micron thickness with a four-step polishing procedure, starting with 220 micron fixed grit diamond plate, then a 45 micron diamond plate. These relatively coarse polishing steps may create debris that is significantly larger than the aperture of all microfractures observed in this study, typically 10 microns or less. After the coarse polish, each section was ultrasonically cleaned with 99.9% isopropyl alcohol and dried on a hot plate. An epoxy layer was then applied to the surface and this was polished with a hand lap and 600 grit (average 20 micron) silica carbide powder, followed by ultrasonic cleaning and 1000 grit (average 5 micron) silica carbide powder. This fine grinding was performed on an epoxy-impregnated surface, minimizing the chance of infilling of microfractures from polishing.

Microfracture density data were determined for each thin section using a petrographic microscope with a flat stage and micrometer. Data were collected from 50 evenly-spaced grid points per thin section. Density was determined by counting the number of fractures that intersected the horizontal crosshair at 20X magnification (corresponding to a field of view of 0.9mm). The microscope stage was rotated an arbitrary amount at each site in order to randomize the counting line orientation. The total number of microfracture intersections was divided by the total counting line length to determine an average linear density of microfractures (microfractures per millimeter).

Microfractures were identified as either open or filled using optical microscopy techniques at 20X magnification. All microfractures counted were sharp-tipped with matching sides and cut across two or more grains (transgranular). Microfractures containing secondary minerals which are optically distinct (color, texture, birefringence) from the crystals that they crosscut are classified as filled (Figure DR1). Microfractures that do not contain any secondary minerals are classified as open (open microfractures appear blue in thin sections that were impregnated with blue-dyed epoxy; Figure DR1a).

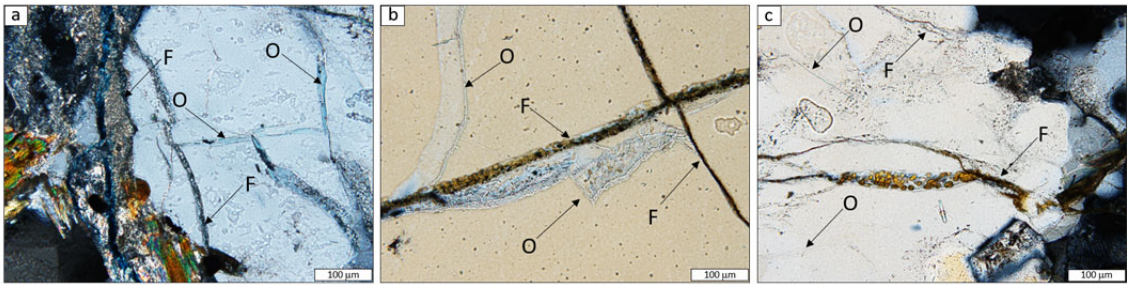


Figure DR1. Examples of open (O) and filled (F) microfractures in quartz crystals from (a) U15n#10, (b) U15n#12, and (c) U15n#13.

## Tables

Table DR1. Sample names, depths, and microfracture densities. Calcite-filled fractures are included in the filled microfracture measurements. Mf, microfracture. U15n samples were collected before any of the SPE explosions; U15n#10 was collected 6 weeks after SPE-2, and U15n#12, and U15n#13 were collected 18 weeks and 21 weeks after SPE-3).

| Sample Name | Vertical Depth (m) | Open Transgranular Mf Density (mf/mm) | Filled Transgranular Mf Density (mf/mm) | Calcite-filled microfractures (mf/mm) |
|---|---|---|---|---|
| u15n_14 | 4.3 | 0.1 | 0.4 | 0 |
| u15n_29 | 8.8 | 0.5 | 0.6 | 0 |
| u15n_50 | 15.2 | 0.2 | 0.5 | 0 |
| u15n_70 | 21.3 | 0.2 | 0.3 | 0 |
| u15n_87 | 26.5 | 0.7 | 1.1 | 0.5 |
| u15n_108 | 32.9 | 0.2 | 0.4 | 0 |
| u15n_132 | 40.2 | 0.1 | 0.2 | 0 |
| u15n_154 | 46.9 | 0.3 | 0.2 | 0 |
| u15n_177 | 53.9 | 0.2 | 0.4 | 0 |
| u15n_192 | 58.5 | 0.3 | 0.2 | 0.2 |
| u15n10_12 | 3.3 | 2.2 | 0.6 | 0 |
| u15n10_24 | 6.6 | 0.9 | 0.4 | 0 |
| u15n10_52 | 13.9 | 0.4 | 0 | 0 |
| u15n10_84 | 22.4 | 0.2 | 0.9 | 0 |
| u15n10_107 | 28.3 | 1.9 | 0.4 | 0 |
| u15n10_116 | 30.6 | 0.3 | 0.2 | 0 |
| u15n10_119 | 31.6 | 0.4 | 0.2 | 0 |
| u15n10_137 | 36.1 | 0.5 | 0.4 | 0 |
| u15n10_143 | 37.6 | 0.5 | 1.5 | 0 |
| u15n10_144 | 38.0 | 1.7 | 4.7 | 0.8 |
| u15n10_148 | 39.1 | 3.0 | 1.7 | 0 |
| u15n10_152 | 40.1 | 4.5 | 3.7 | 0.1 |
| u15n10_155 | 40.9 | 0.3 | 2.6 | 0 |
| u15n10_161 | 42.5 | 0.5 | 0.8 | 0 |
| u15n10_168 | 44.3 | 6.7 | 0.3 | 0 |
| u15n12_11 | 3.0 | 3.7 | 2.7 | 0 |
| u15n12_22 | 5.7 | 2.5 | 1.1 | 0 |
| u15n12_33 | 8.7 | 1.5 | 2.5 | 0 |
| u15n12_57 | 14.9 | 0.4 | 0.2 | 0 |
| u15n12_62 | 16.3 | 0.9 | 0.9 | 0.1 |
| u15n12_75 | 19.8 | 0.4 | 0.7 | 0 |
| u15n12_85 | 22.5 | 1.6 | 4.6 | 0.1 |
| u15n12_90 | 23.6 | 0.8 | 0.9 | 0.1 |
| u15n12_98 | 25.8 | 0.7 | 1.2 | 0 |
| u15n12_107 | 28.2 | 1.0 | 0.6 | 0 |
| u15n12_117 | 30.9 | 0.5 | 0.4 | 0 |
| u15n12_123 | 32.3 | 1.2 | 1.0 | 0.4 |
| u15n12_140 | 37.0 | 0.3 | 2.2 | 0.2 |
| u15n12_149 | 39.3 | 1.2 | 3.1 | 0 |

| | | | | |
|---|---|---|---|---|
| u15n12_158 | 41.6 | 1.6 | 1.6 | 0 |
| u15n12_161 | 42.5 | 3.1 | 1.1 | 0 |
| u15n13_12 | 3.5 | 1.5 | 1.5 | 0 |
| u15n13_24 | 7.4 | 2.5 | 4.6 | 0 |
| u15n13_34 | 10.2 | 1.9 | 3.2 | 0 |
| u15n13_53 | 16.0 | 1.1 | 2.6 | 0 |
| u15n13_78 | 23.6 | 0.7 | 1.4 | 0 |
| u15n13_97 | 29.6 | 0.9 | 1.2 | 0 |
| u15n13_112 | 34.2 | 0.7 | 0.6 | 0 |
| u15n13_114 | 34.6 | 0.5 | 0.9 | 0 |
| u15n13_126 | 38.5 | 1.9 | 4.2 | 0 |
| u15n13_134 | 40.8 | 0.8 | 1.2 | 0 |
| u15n13_148 | 45.2 | 1.4 | 3.5 | 0 |
| u15n13_155 | 47.1 | 1.2 | 1.1 | 0 |
| u15n13_160 | 48.6 | 0.7 | 1.2 | 0 |
| u15n13_180 | 54.9 | 0.2 | 0.3 | 0 |
| u15n13_192 | 58.6 | 0.8 | 1.8 | 0 |
| u15n13_195 | 59.5 | 1.2 | 1.0 | 0 |
| u15n13_209 | 63.6 | 0.5 | 0.4 | 0 |
| u15n13_230 | 70.1 | 0.5 | 0.2 | 0 |
| u15n13_277 | 84.5 | 0.4 | 1.1 | 0 |
| u15n13_283 | 86.4 | 0.4 | 0.8 | 0 |
| u15n13_306 | 93.3 | 0.5 | 1.7 | 0.6 |
| u15n13_325 | 98.9 | 0.8 | 2.2 | 0 |
| u15n13_363 | 110.6 | 0.2 | 0.4 | 0 |
| u15n13_373 | 113.7 | 0.3 | 0.4 | 0 |

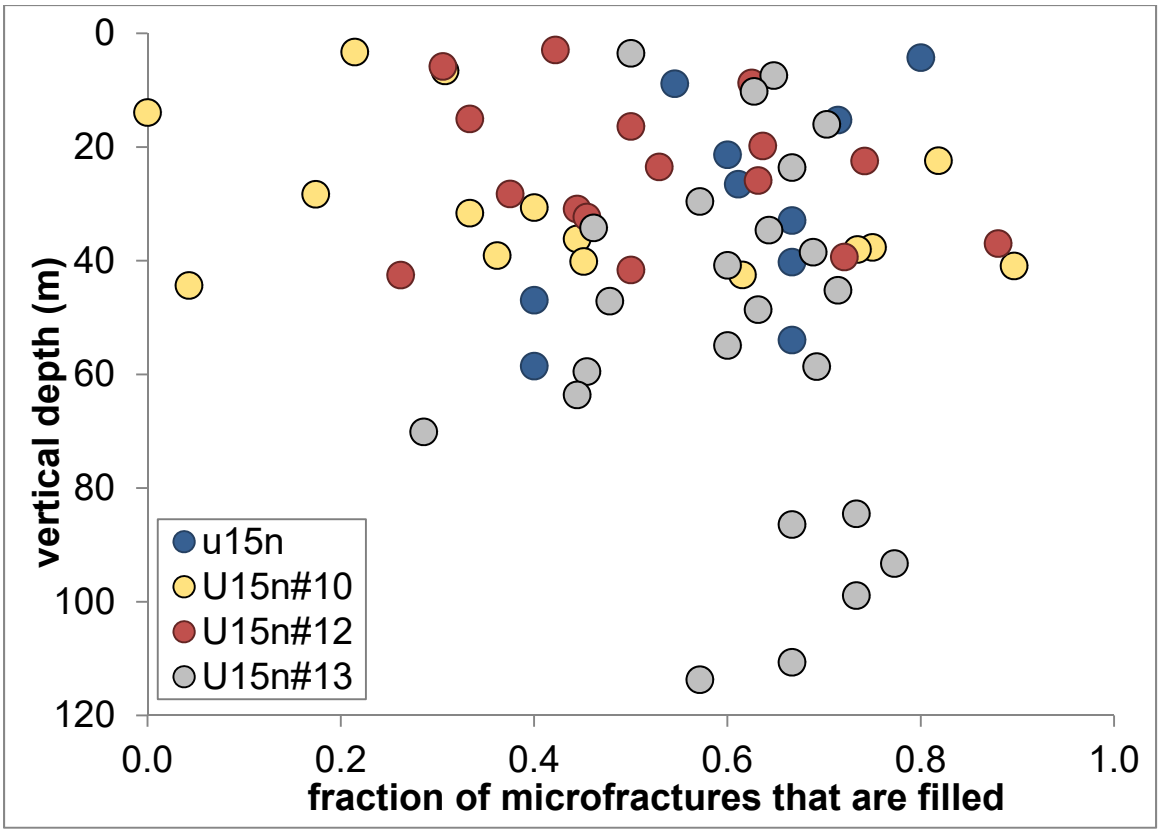


Figure DR2: Plot of the ratio of filled fractures to total transgranular microfractures, as a function of vertical depth of sample. These values are highly variable, particularly for the post-ex samples. The 4 samples that have the lowest fraction of filled microfractures are from the post-ex core collected the soonest after the explosion, U15n#10.